TECHNICAL PAPER

A comparative study of the mechanical and tribological behaviours of different aluminium matrix–ceramic composites

N. Rajesh Jesudoss Hynes[1] · R. Sankaranarayanan[1] · R. Tharmaraj[2] · Catalin Iulian Pruncu[3] · Derya Dispinar[4]

Abstract
Aluminium matrix composites (AMCs) have great potential for critical applications within aerospace, automotive, defence, marine, agriculture and nuclear engineering sectors. The composite materials are very attractive because of their good balance between lightweight versus high strength and machinability. Depending on the particular application, these properties can be further enhanced by adding silicon carbide, boron carbide and graphite, respectively. These reinforcements help to upscale the physical/mechanical properties in order to meet the novel industrial demand. In the present work, a novel hybrid composite is developed through stir cast welding technique. The novel materials manufactured are of great importance, because they exhibit higher mechanical properties and better wear resistance with respect to classical materials (i.e. pure aluminium). The results of mechanical test showed that the addition of 5% boron carbide content to aluminium matrix permits to enhance the tensile properties, shear strength and hardness values; 6% silicon carbide and 4% graphite allow to improve the flexural strength and wear rate, respectively. The best performance was obtained for aluminium composite with 5 wt% boron carbide. The correlation between industrial requirements and the findings from this research indicates that the newly developed composite is an excellent candidate material for structural neutron absorber, armour plate and as a substrate material for computer hard discs.

Keywords Aluminium matrix composites · Boron carbide · Silicon carbide · Graphite · Mechanical properties

Abbreviations

MMCs	Metal matrix composites
MML	Mechanically mixed layer
LM0	Aluminium alloy
AMCs	Aluminium matrix composites
IS	International standard
UTM	Universal testing machine
ASTM	American Society for Testing and Materials
SEM	Scanning electron microscope
TiC	Titanium carbide
SiC	Silicon carbide
B4C	Boron carbide
Al_2O_3	Aluminium oxide
MgO	Magnesium oxide
Gr	Graphite

✉ N. Rajesh Jesudoss Hynes
findhynes@yahoo.co.in

1 Department of Mechanical Engineering, Mepco Schlenk Engineering College (Autonomous), Sivakasi, Tamil Nadu 626 005, India

2 Department of Mechanical Engineering, National Institute of Technology, Warangal, Telangana 506004, India

3 Mechanics of Materials Division, Department of Mechanical Engineering, Imperial College London, South Kensington Campus, London SW72AZ, UK

4 Istanbul Technical University, Metallurgical and Materials Engineering, 34467 Istanbul, Turkey

1 Introduction

The outstanding properties of metal matrix composites (MMCs) have resulted in their substitution for the materials typically employed in a wide range of structural purposes, such as aerospace, defence, sports and transportation industries. They are used to substitute the monolithic alloys that are weak in terms of mechanical properties [1]. The most extensively used ceramic materials to reinforce the matrices are Al_2O_3, SiC, MgO and B_4C [2].

McDanels [3] investigated the aluminium matrix composite features containing discontinuous silicon carbide

reinforcement. It was possible to obtain higher fracture strain by increasing the reinforcement content with a slight loss in ductility. Ralph et al. [4] studied the thermomechanical process and properties of metallic matrix composites. The influence of machining parameters on the surface roughness of MMC was analysed [5]. However, some major inconsistencies in the mechanical properties were detected because the reinforcements were not distributed uniformly in the matrix [6].

A large number of fabrication techniques are currently developed to manufacture the metal matrix composites materials according to specific type of reinforcement. These are primarily produced by compo-casting, stir casting, squeeze casting, liquid metal infiltration and spray co-deposition. Compo-casting process involves the agitation of particulate reinforcement in the semisolid metal. Seo et al. [7] studied the effects of hot extrusion through a curved die to improve the mechanical properties of SiC/Al composites fabricated by melt stirring. Xu et al. [8] produced particulate metal matrix composites with a low particulate (SiC and carbon) volume fraction by liquid metal infiltration. Seo et al. [9] prepared SiC/Al composites under squeeze casting conditions for different applied pressures of 70, 100 and 130 MPa. Rajan et al. [10] studied the effect of reinforcement coatings and investigated the bonding mechanism of interfaces in aluminium metal matrix composites. The properties and morphology of fine grains of fly ash incorporated into a composite Al/Si alloy via three distinct stir casting methods have been investigated by Rajan et al. [11]. The study indicated that shearing of the fly ash grains resulted in more effective dispersion and separation of the grains by the compo-casting approach relative to the liquid metal stir casting method. Rosso [12] presented a work on ceramic and metal matrix composites, which were focused on different technologies that provide perspective applications of advanced ceramics, metal matrix and ceramic matrix composites. In the case of metal matrices composites, aluminium and titanium are the principle base materials as reviewed by Rosso, whereas boron carbide, glass–ceramic, alumina, silicon carbide, silicon nitride, etc., are the main constituents for ceramic matrices composites. High homogeneity is required to obtain the optimum mechanical properties of composite materials. Therefore, it is paramount important to control the process parameters. If a high-quality composite is to be obtained, the process control needs to be recognized and remedied. A study on intensive shearing during production of cutting-edge metal matrix composites incorporating Al/SiC particles was performed by Tzamtzis et al. [13]. The study indicated that the rheocasting (semi-molten stir casting) method facilitates the production of greatly enhanced composites via dispersion of the SiC particles. Aybarc et al. [14] studied the use of ultrasonic vibration on the distribution of reinforcements in the matrix. It was found that mechanical stirring followed by ultrasonic vibration (which was called as hybrid stirring) resulted in homogeneous distribution. Aybarc et al. [14] used numerical modelling as well. Hashim et al. [15] investigated the effect of stirrer position in the crucible and stirring speed, which can affect the flow pattern of particles. Although the dispersion of reinforcing particles within the molten matrix can be optimized with the aid of computer modelling and experimental validation, non-uniform distribution remains one of several difficulties surrounding the production of reinforced composite materials. Other problems associated with the present methodologies include particle agglomeration within the ductile matrix leading to a significant reduction in ductility [16, 17]. The microstructure is a very important parameter which influences the properties of the composite. The trial and error methods proposed early in the industry were later confronted by scientific-based techniques. This method was developed by Rabiei et al. [18] to evaluate experimentally aluminium matrix composites with various particle reinforcements. They determined the fracture toughness and compared the experimental results against the fracture toughness estimates using the Hahn–Rosen field model. Due to the good agreement with the experimental findings, it was possible to produce a modified numerical fracture model. Processing maps have been produced by Murty et al. [19] from studies on the hot-working properties of 6061Al MMCs reinforced with SiC and Al_2O_3 particles. Based on the Ziegler's continuum principles, imposing a simple instability condition allows to assess the extent of plastic deformation in a given workpiece. In order to limit the quantity of waste requiring careful disposal, a novel category of MMCs termed ash alloys or syntactic foams has been developed. These consist of Al and Mg alloys reinforced with fly ash [20–22]. For example, in the electrical industry the MMCs that are manufactured from aluminium and magnesium are energy intensive. Therefore, the replacement of an aluminium or magnesium part by fly ash provides significant energy savings [23, 24]. Both the electrical and mechanical properties of MMCs are compromised by reinforcement agglomeration, inhomogeneous distribution and limited wettability during processes such as spray forming, stir casting, squeeze casting and powder metallurgy. Moreover, the costly equipment and intricate processing involved in these techniques result in significant production costs for MMCs. Accumulative roll bonding (ARB) process was used to develop Al/B_4C composites, in which the particles were distributed evenly throughout the matrix without the effect of agglomeration [25]. Sharifi et al. [26] addressed these challenges by using the ball milling technique to mix pure aluminium with various quantities of B4C nanoparticles to generate a range

of Al–B_4C powders. These were then used to generate bulk nanocomposite materials via hot pressing. The hardness, ultimate compressive strength and wear resistance of the nanocomposites were increased significantly by increasing the B_4C content in pure aluminium powder. Toptan et al. [27] investigated the processing linked to microstructural characterization of AA 1070 and AA 6063 matrix B_4Cp-reinforced composites. Such Al–B_4C materials have also been produced by other methods, including powder metallurgy (solid-state consolidation) and liquid-phase techniques [28]. The tribological and mechanical properties of aluminium matrix composites can be enhanced by reducing the size of the reinforcement particles to the nanometre scale [29]. Metal–metal contact is effectively avoided by the development of an insulating mechanically mixed layer (MML). A higher reinforcement content in the nanocomposite promotes stronger material transfer from the counterface generating the oxidation reaction. This leads to more rapid development, enhanced thickness and increased oxide content of the protective MML during wear, thus decreasing the rate of wear [30].

Therefore, the advanced manufacturing methods of MMCs presented here offer effective solution in order to form novel material with better mechanical properties (i.e. higher hardness, ultimate compressive strength and wear resistance) that suit the industrial needs. But, none of them consider the base metal as aluminium alloy (LM0) which has low machinability and high resistance to corrosion. This paper proposes a robust experimental approach focused on hybrid reinforcements of pure aluminium which allows enhancement of the mechanical properties of the composites and promotes better wear resistance. The aluminium alloy (LM0) as base metal was used to produce novel MMC using a hybrid reinforcement procedure. Different percentages of silicon carbide, boron carbide and graphite as powder form were used to reinforce aluminium matrix to obtain the best mechanical and tribological properties.

2 Materials and processing methods

2.1 Selection of matrix and its constituents

In this research, in order to produce the metal–matrix composite, aluminium alloy (LM0) was selected as the base matrix material, while silicon carbide, boron carbide and graphite were used as the reinforcers. The reinforcements had an average mesh size of 220 nm in the form of powders. Chemical composition of LM0 and material properties of matrix with its constituents are given in Tables 1 and 2, respectively.

2.2 Stir casting

The stir casting is a primary process developed to produce the composite. In this routine, the reinforcements are mixed into the molten base metal with continuous stirring, followed by transfer to the die for solidification. Strong stirring at elevated temperature is the only way to break down the agglomerates that frequently develop during stir casting. The benefits of stir casting include its flexibility, ease of operation and control of matrix structure, applicability to large-scale processing, production of pieces close to the required final shape (near net shaping) and low processing cost. The stir casting method used in this survey allows preparing an optimal composition of aluminium metal–matrix composite. The test set-up is given in Fig. 1. A range of uniform, high-strength aluminium composite materials have thus can be produced by using the whirlpool technique.

Table 1 Chemical composition of LM0

	Copper	Magnesium	Silicon	Iron	Manganese	Nickel	Zinc	Lead	Tin	Aluminium	Others: total
Max. %	0.03	0.03	0.30	0.40	0.03	0.03	0.07	0.03	0.03	99.50[a]	0.50

[a]Maximum (Max.) % of aluminium content refers the percentage excluding the total of all other elements

Table 2 Summary of material properties

Material	Tensile strength (MPa)	Density (g/cm^3)	Coefficient of thermal expansion (/°C)	Modulus of elasticity (GPa)
Aluminium alloy LM0 (grade)	80	2.70	2.85×10^{-5}	69
SiC	34.48–137.9	3.1	4.0×10^{-6}	410
B_4C	261	2.3–2.55	3.2×10^{-6}	362
Gr	29.1	1.3–1.95	$1.2–8.2\times10^{-6}$	8–15

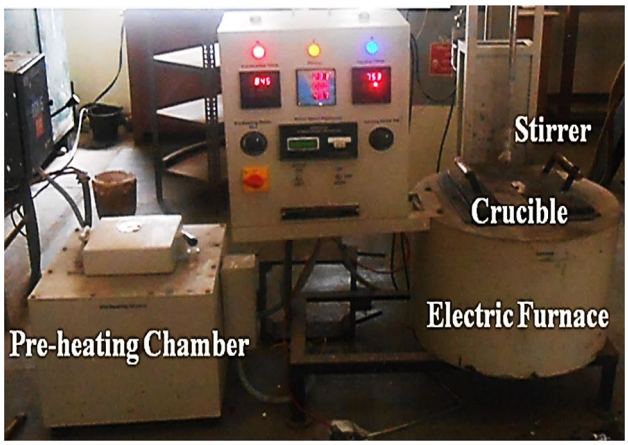

Fig. 1 Main components settled to fabricate the MMCs by stir casting method

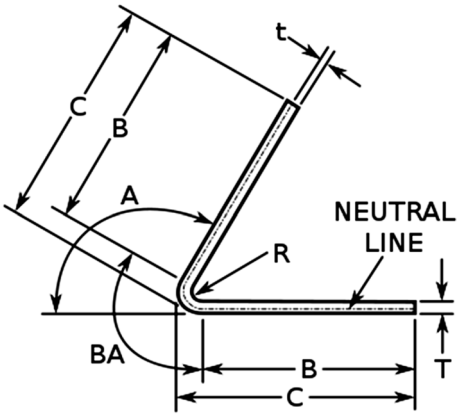

Fig. 2 Bend terminology used for a general angle, *BA* bend allowance, *R* inner bend radius, *T* part thickness, *t* distance between inner face and neutral line, *A* material bending angle (°), *B* span of flange, *C* mould line dimension

2.3 Production of AMCs

The furnace components and four mild steel stirrer blades comprised the experimental set-up. In the first step, the empty crucible and the boron carbide, silicon carbide and graphite powders were separately preheated close to the main processing temperature. The aluminium ingot (95% pure) was then subjected to melting at 830 °C in the graphite crucible within the furnace, while the preheated powders were mechanically mixed together below their melting points. Initially, the ingot was preheated for 3–4 h at around 550 °C. At the same time silicon carbide, boron carbide and graphite powders were preheated to 850–900 °C in the preheating furnace. The metal matrix was held at the same temperature in the furnace to permit complete mixing of the boron carbide, silicon carbide and graphite powders into the molten aluminium. Uniform dispersion of the powders throughout the aluminium alloy matrix was facilitated by lowering the stirring mechanism into the crucible (inside the furnace) to the appropriate depth allowing 10 min of vigorous automatic stirring at 550 rpm. The test rig used in the present work can be shown in Fig. 1. In the final mixing process, the temperature rate of the furnace was kept at 830 ± 10 °C. Any gases trapped in the mixture are completely removed by the degasser, thereby preventing easy transfer of heat from the mixture to the atmosphere. The above experiment was performed several times with different composite powder compositions, keeping the total mass of mixture at 1500 g in each case. The capacity of the die for the stir casting is 1800 g. Hence, the total mass mixture was taken as 1500 g in accordance with the capacity of the die. For a better homogenization of the composition, the samples were melted and solidified in two dies. The outer diameter and length of the die are 20 mm and 200 mm, respectively.

The samples produced in this paper were indicated as: sample 1 that contains LM0 90%, silicon carbide 6% and graphite 4% [31, 32], sample 2 that contains LM0 90% and silicon carbide 10% [31] and sample 3 form of LM0 95% and boron carbide 5% [33].

3 Assessment of novel material performances

To prove consistency in the results for each type of test versus sample, at least six simulations were performed.

3.1 Tensile tests

In order to determine the material ability to resist to diffident mechanical loadings (e.g. static and dynamic load), a classical tension or compression test is compulsory. It allows to evaluate its fundamental mechanical properties (i.e. the yield stress and tensile strength). Besides, using a general tensile test permits to control the quality of materials used in design processes. The specimens were prepared in accordance with ASTM: B-557M standards [34].

3.2 Flexural test

The bending performances of novel composite were evaluated using a flexural test. The flexural tests were performed under the three-point flexural testing machine. It entails to determine the behaviour of materials subjected to simple bending loads. The specimen was prepared in accordance with IS: 1599 standards [35, 36]. During the bending operation, the material located near of the bend radius is under compression while the material near the outside of the bend

is under tension (see details in Fig. 2). A neutral plane exists between the area under tension and area under compression. When a blank or sheet is bended, it is necessary to consider the effect of stretching the metal at the outside of the bend. Since there is no stretch in the neutral plane, the length of the formed part along the neutral plane will be the correct length. Through curved neutral plane of the bend area, bend allowance (BA) can be calculated. The blank length dimensions evaluated on the test specimen before and after bend test are given in Table 3.

3.3 Impact test

The impact test permits to estimate the material resistance to sudden and dynamic loadings of the composite specimen. Applying this test method is possible to measure the amount of energy absorbed (in joules) by the specimen during the rupture. A classical Charpy impact test was carried out. The specimen was prepared in accordance with IS: 1757 standards [37].

3.4 Hardness test

In the present work, the level of deformation displayed by the new composite materials when subjected to constant compressive load by a very sharp object was evaluated according to the Micro Vickers hardness test. The specimen was prepared as per IS: 1501 standards [38]. Indentation were made on the specimen, with an applied load of 0.5 kg.

3.5 Shear test

The shear test was carried out by FIE make Universal Testing Machine (UTM). The model number is UTN 40, and its serial number is 11/98-2450. Machine is made in India. As per ASTM: 831-05 standard, [39] prepared the samples and conducted the shear test.

3.6 Wear test

The wear test was carried out using a pin-on-disc equipment. The test simulation was performed in dry condition to replicate the dry sliding wear. The tests were conducted for different numbers of specimens on a machine supplied by DUCOM (Model: Wear & Friction Monitor TR-20). The specimen was prepared as per ASTM: G-99 standards [40]. The wear test parameter values are introduced in Table 4. The wear rate of novel composite material was calculated as a difference between the weight of the specimen before trial and measured weight after each test using a balance (up to an accuracy of 0.0001 g using microbalance).

Table 4 Parameters' condition for the wear test

Parameters	Value
Load (kg)	1
Sliding distance (m)	1000
Speed (m/s)	3.145
Rotational speed (rpm)	500
Total time (min)	5.30

3.7 Morphological analysis by scanning electron microscope (SEM)

The scanning electron microscope (SEM) is considered an advanced tool to detect the quality of material produced. During the SEM measurements, the materials surface is submitted to electrons bombarding which by reflection allows to form an image. The sample holder stub was cleaned with acetone and dried in the sputter coater machine using 240 V. The sample was prepared and proceeded to analyse its microstructure in the SEM.

4 Results and discussion

4.1 Tensile test

Figure 3 shows the comparison of the force versus stroke for the three samples produced by reinforcements. It can be noted that sample 3 that contains aluminium alloy (LM 0) 95% and boron carbide 5% has the highest value of force for the same values of stroke; its values are followed by sample 1 and sample 2. The comparison of yield stress,

Table 3 Blank length of the test specimen before and after bending test

Sample	Composition of composite specimen	Before bending (mm)	After bending (mm)
Sample 1	Aluminium alloy (LM 0) 90% Silicon carbide 6% Graphite 4%	150	152.9
Sample 2	Aluminium alloy (LM 0) 90% Silicon carbide 10%	150	151.094
Sample 3	Aluminium alloy (LM 0) 95% Boron carbide 5%	150	153.046

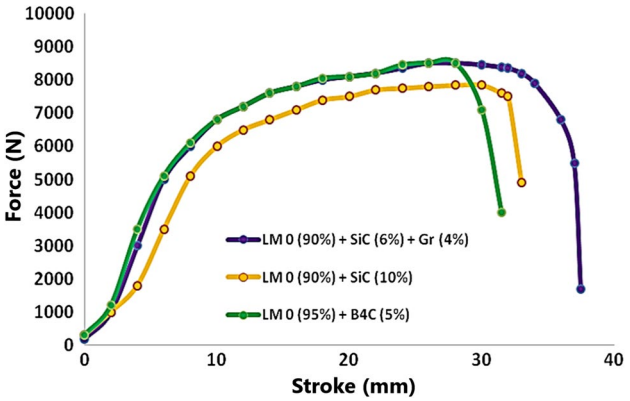

Fig. 3 Force versus stroke evolution from the tensile test results

ultimate tensile strength and elongation percentage for the three materials produced is plotted in Fig. 4.

The sample 3 has a greater yield stress (~ 43 MPa) followed by sample 2 (~ 42 MPa) and sample 1 (~ 41 MPa), and it is because of high percentage of base metal and its specific reinforcement (i.e. boron carbide). Further, sample 3 has greater ultimate tensile strength (~ 71 MPa) followed by sample 1 (~ 70 MPa) and sample 2 (~ 70 MPa).

Tensile strength of LM0 is 80 MPa. However, the addition of reinforcements in samples 1 and 3 leads to decrease in the tensile strength by 13.4% and 9.5%, respectively. A potential reason for higher tensile strength in the sample 3 is linked to the boron carbide features that have a high strength and, of course, the LM0 percentage that is higher compared to the other two samples. Sample 1 has the maximum values elongation (cc. 46%) followed by sample 2 (cc. 38%) and sample 3 (cc. 35%). It proves the role of reinforcements added to the base metal. A summary of tensile properties of novel composited materials is given in Table 5.

Table 5 Tensile properties of novel composites

Sample	Break load (KN)	Tensile strength (MPa)	Elongation (%)	Yield stress (MPa)
Sample 1	8.50	69.27	45.60	41.79
Sample 2	7.84	64.93	37.60	42.83
Sample 3	8.51	70.47	34.40	42.86

4.2 Flexural test

Figure 5 provides details of the specimen prepared for flexural test and general view of specimen after testing.

An overview of flexural properties achieved from the novel produced composite is given in Table 6.

The evolution of force versus stroke graph representing the flexural simulation is presented in Fig. 6. It can be noted that sample 1 has the highest value of force (~ 4.36 kN) for the same values of stroke. The numerical values of flexural behaviour of sample 3 and sample 2 were found slightly lower (~ 3.99 and 3.59 kN, respectively). Sample 1 proves a greater flexural strength (~ 12.67 N/mm^2) and slightly higher compared to sample 2 (~ 12.09 N/mm^2) and sample 3 (~ 9.34 N/mm^2). It is due to the addition of silicon carbide and graphite within LM0 compound. Besides, the deflection was higher in sample 3 (~ 3.04 mm) when compared to sample 1 and sample 2 (~ 2.09 and 1.09 mm, respectively).

4.3 Impact test

Figure 7 presents details of the prepared specimens (Fig. 7a) and specimens after the impact test (Fig. 7b). The summary of the results achieved from the impact test is presented in Table 7. As can be seen, samples 1 shows better properties which permit absorbing large amount of energy (up to 56 J). The other two samples reveal a much lower energy features, as sample 2 (~ 28 J) and sample 3 (only 12 J).

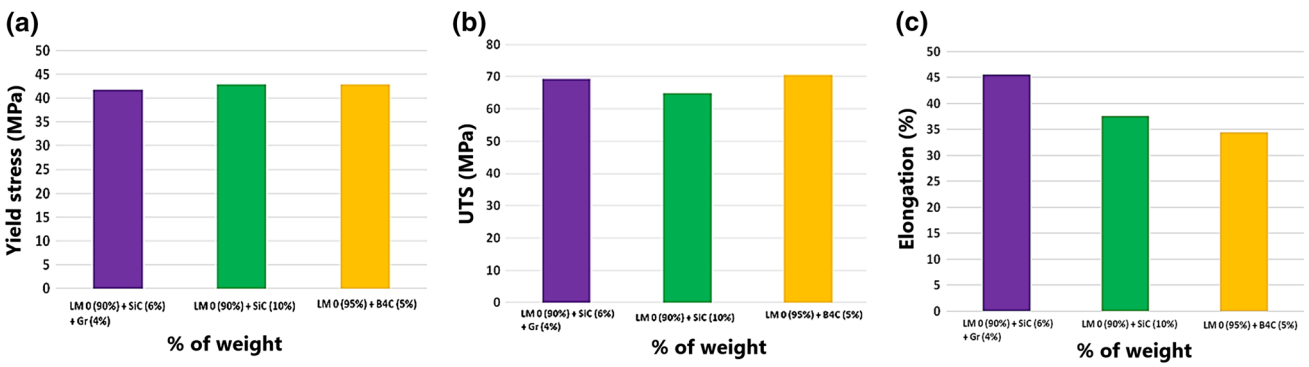

Fig. 4 Mechanical properties as per tensile test: **a** material yield stress (%), **b** ultimate tensile strength (MPa) and **c** elongation performances (%)

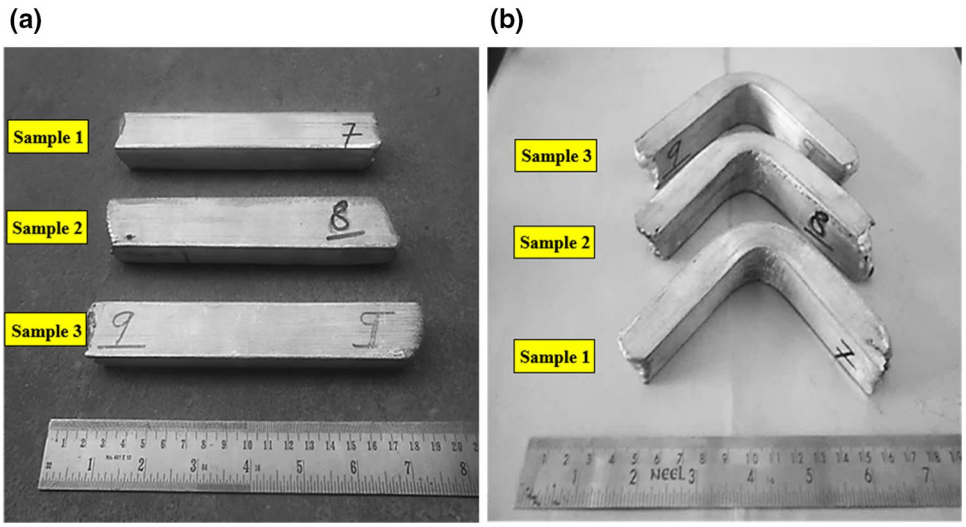

Fig. 5 Details of bend specimens **a** before and **b** after test

Table 6 Flexural properties of novel composites produced

Sample	Flexural break load (kN)	Maximum deflection (mm)	Flexural strength (N/mm^2)
Sample 1	4.36	2.9	12.674
Sample 2	3.59	1.094	9.348
Sample 3	3.99	3.046	12.09

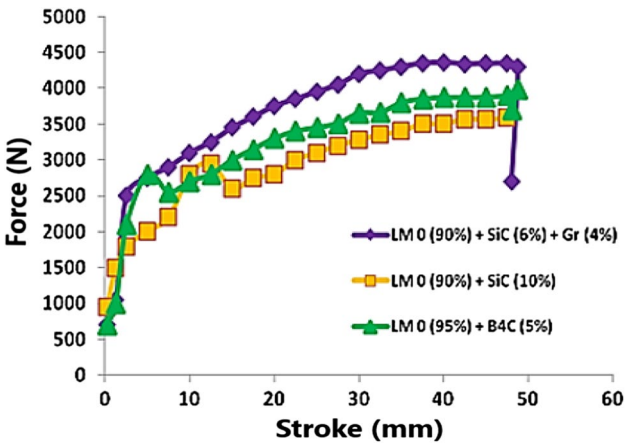

Fig. 6 Evolution of force versus stroke after the flexural test

Here, the two reinforcements (SiC and Gr) seem to play a great role as the additives into the base metal (LM0), as no fracture was observed in that sample.

4.4 Micro Vickers hardness test

The Micro Vickers hardness test was carried out on the samples produced, three times for each sample, and the results are given in Table 8.

The results show better properties in terms of hardness for sample 3 which indicates a maximum hardness of 88.43 HV. The other two samples demonstrate much lower values. Hence, sample 2 shows 27.93 and sample 1 has almost a similar value of 27.26 HV. The reason for the increase in the hardness can be attributed to the reinforcement by B_4C that were mixed within the base metal (LM0).

4.5 Shear test

The geometrical shear samples and pattern of its fracture are given in Fig. 8. Further, Fig. 9 shows the evolution of force versus stroke graph for three different types of samples produced.

Table 9 presents an overview with the results achieved. The shear strength of novel composite materials presents comparable numerical values with sample 3 having the highest value (~ 54.25 N/mm^2). It is apparent that the boron carbide reinforcement added into the base metal of LM0 generates better properties.

4.6 Wear test

Figure 10 shows details of tribological evolution. The friction force versus time is plotted in the graph of Fig. 10a. Further, in Fig. 10b the evolution of wear against time for the three different specimens produced is plotted. Wear rate evolution for the tested samples is given in Table 10.

It can be noted that sample 2 has the highest value of frictional force followed by sample 1 and sample 3, while

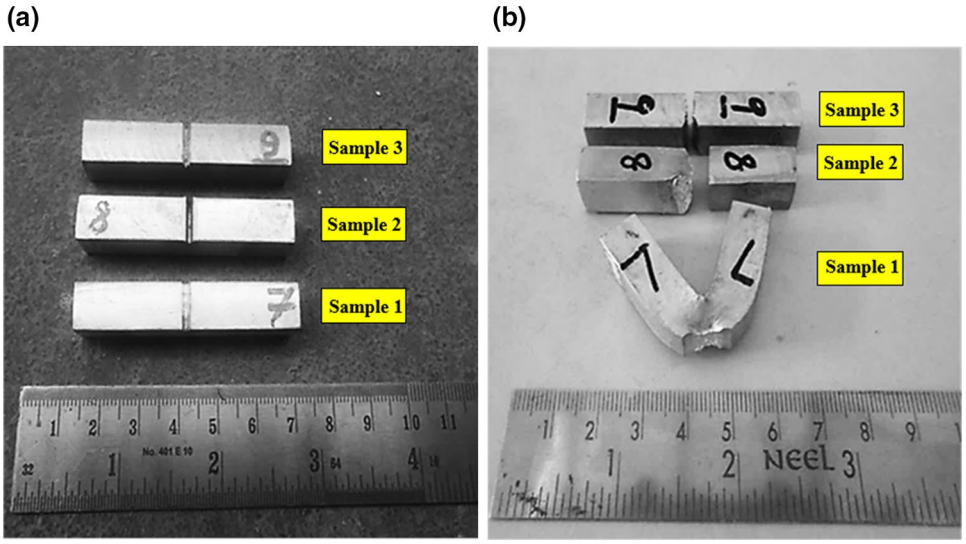

Fig. 7 The impact specimen **a** before and **b** and after impact test

Table 7 Impact properties of novel composites

Sample	Energy absorbed (J)
Sample 1	56
Sample 2	28
Sample 3	12

Table 8 Hardness values of novel composites [in HV]

Sample	Trail 1 (HV)	Trail 2 (HV)	Trail 3 (HV)	Average hardness (HV)
Sample 1	27.20	27.30	27.30	27.26
Sample 2	27.70	28.60	27.50	27.93
Sample 3	90.90	96.20	78.20	88.43

in terms of wear rate sample 3 (~ 0.0299 g) has the highest value of wear followed by sample 2 (~ 0.0248 g) and sample 1 (~ 0.0081 g).

The results demonstrate that the use of a specific volume fraction of B_4C allows to enhance the UTS and hardness of the composite. Potentially, if it is increased further, the amount of volume fraction of B_4C having much better properties can be obtained [41].

SiC content was found to be homogeneously distributed in the microstructure. Therefore, by adding some amount of SiC content in Al matrix the hardness and its tensile strength of AMCs were increased compared with unreinforced [42]. However, it can have some detrimental effects on the elongation performances and impact strength of novel composites that agrees with observation made by adding TiC [43]. Figure 11 presents a picture with the tensile test specimens post-mortem.

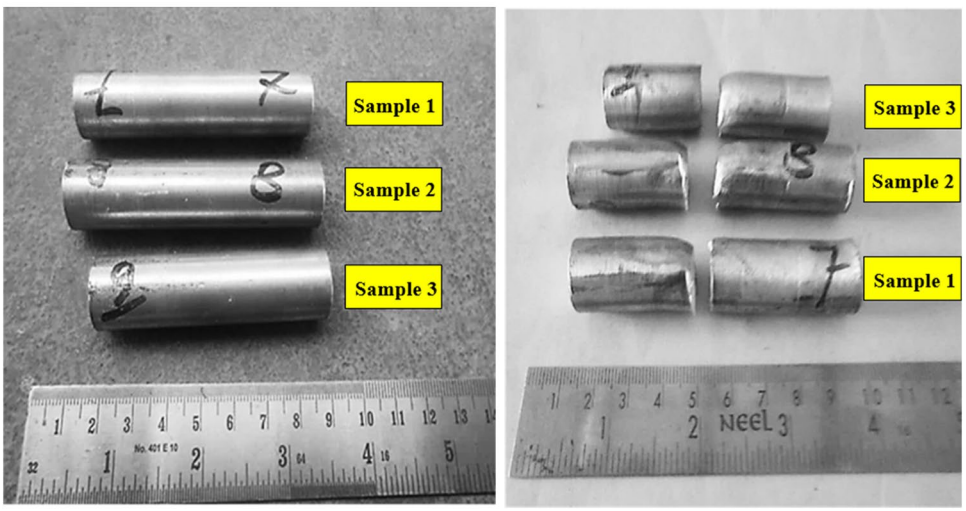

Fig. 8 **a** Specimen prepared for shear test and **b** specimen post-mortem

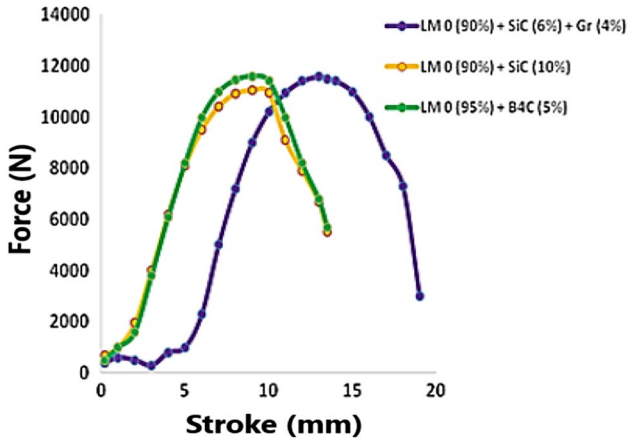

Fig. 9 Shear material behaviour during loading conditions

Table 9 Shear values of novel composites

Sample	Shear load (kN)	Shear strength (N/mm^2)
Sample 1	11.57	54.11
Sample 2	11.04	51.63
Sample 3	11.60	54.25

The nanoparticles added in the matrix can help protecting the surface by forming an oxide layer which promotes a better wear resistance. Probably, this oxide layer is generated as an interfacial reaction that produces the Al_3BC phase with direct effect on the interfacial characteristics [44]. Besides, it was proved that the addition of nanoparticles to the matrix of aluminium permits to increase the hardness [45]. Therefore, a limited amount of graphite and/or nano-/micro-B_4C particles can produce better properties in terms of wear resistance [46, 47].

Figure 12 depicts the morphological microstructure of the novel composite produced. Clusters of silicon carbide and graphite are observed in some places as depicted in Fig. 12a of sample 1 that is due to the agglomeration effect. However, this seems detrimental to the strength of the composites. Silicon carbide particles were observed along with white inclusion which is stir casting defect. The inclusion can further generate some porosity as observed in Fig. 12b and analysed from sample 2.

Sample 3 lower wear rate is linked to the high hardness and strength of boron carbide that presents inferior properties in abrasive resistance [48], therefore promoting lower wear resistance. Further, the higher weight loss of composite from sample 2 during the ball-on-disc test could be caused by the abrasive wearing due to micro-cutting or ridging along with spalling of SiC hard particles out

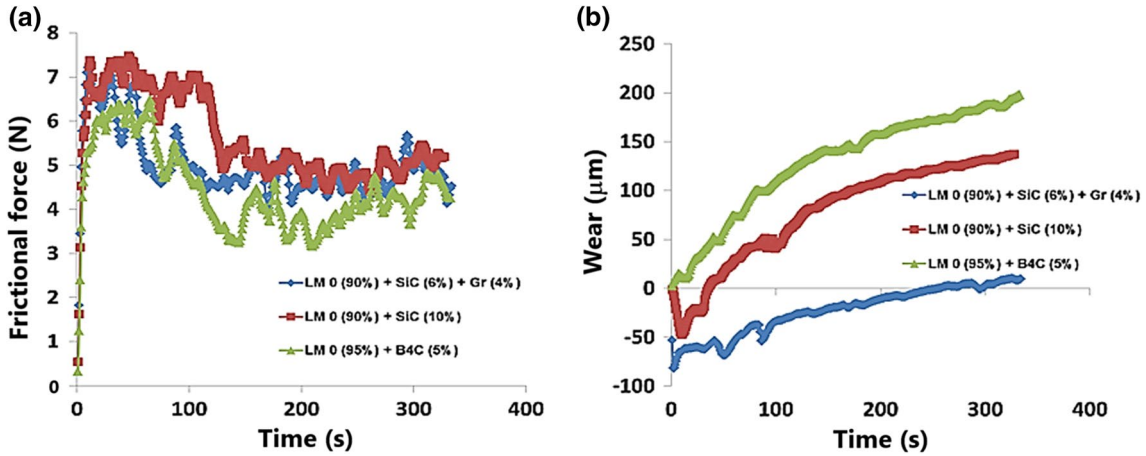

Fig. 10 Results of tribological test for the three compositions: **a** frictional force versus time and **b** wear versus time

Table 10 Wear rate evolution for the samples tested

Sample	Weight before wear test (g)	Weight after wear test (g)	Wear rate (g)
Sample 1	9.0776	9.0696	0.008
Sample 2	8.8528	8.8280	0.0248
Sample 3	7.8009	7.7710	0.0299

of the composite matrix (intensifying the wear process) [49]. Analysis of the sample 3 proves the distribution of boron carbide evenly throughout the aluminium matrix (see Fig. 12c). The uniform dispersion occurs as the particles are distributed between the dendrite boundaries into small-scale clustering and agglomeration of B_4C [49]. It was noted that B_4C content into the Al matrix reveals a superior impact on the mechanical properties of samples

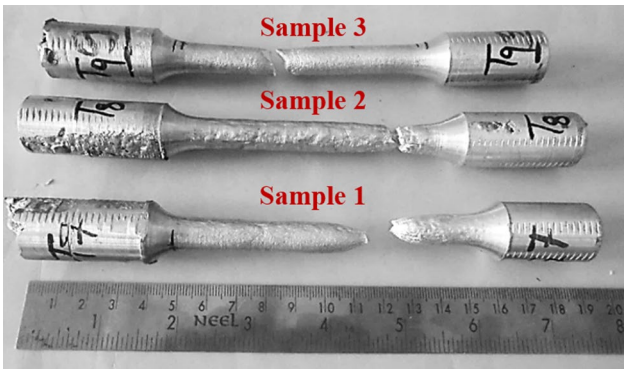

Fig. 11 Patterns of tensile specimens after the tensile test

until wettability is not affected by the particles volume fraction [40].

The novel material formed as ceramic/aluminium composite can resist better to external loads, due to superior interfacial ceramic/aluminium bonding effect caused by the movement of grain and twin boundaries [50]. It is envisaged that it could be effectively employed in defence applications compatible with new joining technologies [51, 52].

In the future research, we intend to introduce in a small percentage the agro-waste and some advanced optimization strategies to determine the optimum processing parameters in order to generate a recycling cycle. The hybrid AMCs reinforced with agro-waste derivatives prove its economic benefits because it allows reduction of the production cost even at about 50% when used to replace the synthetic reinforcement with the agro-waste.

5 Conclusions

This work presents a robust assessment of a novel material composite manufactured using different percentages of reinforcements; therefore, three different types of samples are fabricated and then analysed for their mechanical features. The following conclusions were drawn:

- Tensile strength of composite formed by mixing 5% B_4C with the LM0 is marginally higher with respect to LM0 with 6% silicon carbide and 4% graphite and/or LM0 with 10% silicon carbide, respectively, caused by a homogenous distribution of the volume fraction of B_4C;
- Impact and flexural strength of LM0 with 6% silicon carbide and 4% graphite are higher than LM0 with 10% silicon carbide and LM0 with 5% B_4C, respectively. Probably, the silicon and graphite content promotes superior toughening mechanisms which make the composite to resist better to such kind of loadings;
- The hardness properties of LM0 with 6% silicon carbide and 4% graphite are comparable to the LM0 with 10% silicon carbide; however, the values are only half of composite LM0 with 5% B_4C. Despite of this, the wear rate does not have the same trend nevertheless. However, we have not achieved a correlation between hardness and wear rate. In terms of wear, the LM0 with 6% silicon carbide and 4% graphite proves better properties with respect to LM0 with 10% silicon carbide and LM0 with 5% B_4C, respectively.

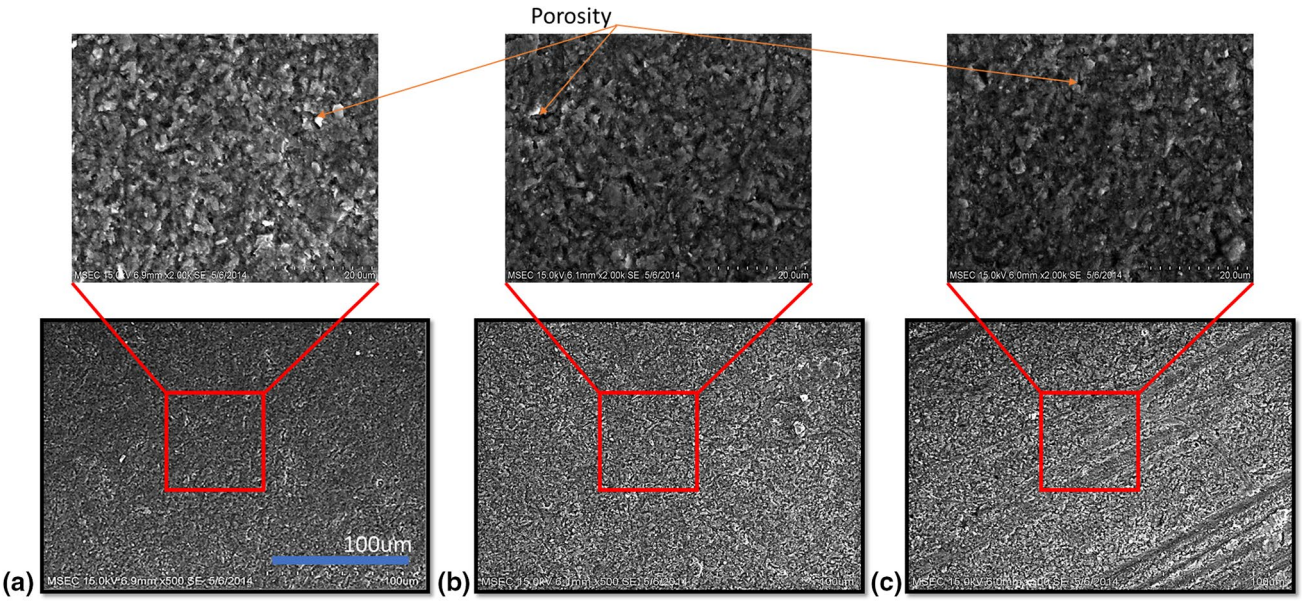

Fig. 12 Morphological microstructure of novel composite **a** samples 1, **b** sample 2 and **c** samples 3

- The shear results do not depend on the reinforcement type studied here as they shows quite similar numerical values.

In the future work in order to validate the manufacturing robustness, we intend to produce larger and industrial components for structural neutron absorber, armour plate and as a substrate material for computer hard discs.

Acknowledgements The authors gratefully acknowledge the financial support of this work by SERB of Department of Science and Technology, New Delhi, India (Vide Letter No.: SERB/F/1452/2013-2014, dated 10.06.2013), and author R. Sankaranarayan is grateful for the award of PhD fellowship by Mepco Schlenk Engineering College (Autonomous), Sivakasi, 626005, Tamilnadu, India (Vide Letter No.: OF/GT/F01/5309/2017-2018, dated 13.03.2018).

References

1. Panwar N, Chauhan A (2018) Fabrication methods of particulate reinforced aluminium metal matrix composite: a review. Mater Today 5(2, Part 1):5933–5939
2. Mavhungu ST, Akinlabi ET, Onitiri MA, Varachia FM (2017) Aluminum matrix composites for industrial use: advances and trends. Procedia Manuf 7:178–182
3. McDanels DL (1985) Analysis of stress–strain, fracture, and ductility behavior of aluminum matrix composites containing discontinuous silicon carbide reinforcement. Metall Trans A 16(6):1105–1115
4. Ralph B, Yuen HC, Lee WB (1997) The processing of metal matrix composites: an overview. J Mater Process Technol 63(1):339–353
5. James SJ, Venkatesan K, Kuppan P, Ramanujam R (2014) Hybrid aluminium metal matrix composite reinforced with SiC and TiB_2. Procedia Eng 97:1018–1026
6. Afkham Y, Khosroshahi RA, Rahimpour S, Aavani C, Brabazon D, Mousavian RT (2018) Enhanced mechanical properties of in situ aluminium matrix composites reinforced by alumina nanoparticles. Arch Civ Mech Eng 18(1):215–226
7. Seo YH, Kang CG (1999) Effects of hot extrusion through a curved die on the mechanical properties of SiCp/Al composites fabricated by melt-stirring. Compos Sci Technol 59:643–654
8. Xu Y, Chung DDL (1998) Low-volume-fraction particulate preforms for making metal–matrix composites by liquid metal infiltration. J Mater Sci 33(19):4707–4709
9. Seo Y-H, Kang C-G (1995) The effect of applied pressure on particle-dispersion characteristics and mechanical properties in melt-stirring squeeze-cast SiCp/Al composites. J Mater Process Technol 55(3):370–379
10. Rajan TPD, Pillai RM, Pai BC (1998) Reinforcement coatings and interfaces in aluminium metal matrix composites. J Mater Sci 33:3491–3503
11. Rajan TPD et al (2007) Fabrication and characterisation of Al–7Si–0.35Mg/fly ash metal matrix composites processed by different stir casting routes. Compos Sci Technol 67(15):3369–3377
12. Rosso M (2006) Ceramic and metal matrix composites: routes and properties. J Mater Process Technol 175(1):364–375
13. Tzamtzis S, Barekar NS, Babu NH, Patel J, Dhindaw BK, Fan Z (2009) Processing of advanced Al/SiC particulate metal matrix composites under intensive shearing: a novel Rheo-process. Compos A Appl Sci Manuf 40(2):144–151
14. Aybarc U et al (2019) The use of stirring methods for the production of SiC-reinforced aluminum matrix composite and validation via simulation studies. Int J Metalcast 13(1):190–200
15. Hashim J, Looney L, Hashmi MSJ (2002) Particle distribution in cast metal matrix composites—part I. J Mater Process Technol 123(2):251–257
16. Deng X, Chawla N (2006) Modeling the effect of particle clustering on the mechanical behavior of SiC particle reinforced Al matrix composites. J Mater Sci 41(17):5731–5734
17. Segurado J, González C, Llorca J (2003) A numerical investigation of the effect of particle clustering on the mechanical properties of composites. Acta Mater 51(8):2355–2369
18. Rabiei A, Vendra L, Kishi T (2008) Fracture behavior of particle reinforced metal matrix composites. Compos A Appl Sci Manuf 39(2):294–300
19. Murty SVSN, Rao BN, Kashyap BP (2003) On the hot working characteristics of 6061Al–SiC and 6061–Al_2O_3 particulate reinforced metal matrix composites. Compos Sci Technol 63(1):119–135
20. Bieniaś J, Walczak M, Surowska B, Sobczak J (2003) Microstructure and corrosion behaviour of aluminum fly ash composites. J Optoelectron Adv Mater 5:493–502
21. Rohatgi PK, Guo RQ (1997) Low cost cast aluminum–fly ash composites for ultralight automotive application. TMS annual meeting, pp 157–168
22. Zhang XF, Wang DJ, Xie G (2002) Manufacturing of aluminum/fly ash composite with liquid reactive sintering technology. Acta Metall Sin (Engl Lett) 15:465–470
23. Rohatgi PK, Guo R, Keshavaram BN, Golden DM (1996) Cast aluminum, fly ash composites for engineering applications. Am Foundrymen's Soc 103:575–580
24. Rohatgi PK, Gajdardziska-Josifovska M, Robertson DP, Kim JK, Guo RQ (2002) Age-hardening characteristics of aluminum alloy–hollow fly ash composites. Metall Mater Trans A 33(5):1541–1547
25. Yazdani A, Salahinejad E (2011) Evolution of reinforcement distribution in Al–B_4C composites during accumulative roll bonding. Mater Des 32(6):3137–3142
26. Sharifi EM, Karimzadeh F, Enayati MH (2011) Fabrication and evaluation of mechanical and tribological properties of boron carbide reinforced aluminum matrix nanocomposites. Mater Des 32(6):3263–3271
27. Toptan F, Kilicarslan A, Karaaslan A, Cigdem M, Kerti I (2010) Processing and microstructural characterisation of AA 1070 and AA 6063 matrix B_4Cp reinforced composites. Mater Des 31:S87–S91
28. Lashgari HR, Zangeneh S, Shahmir H, Saghafi M, Emamy M (2010) Heat treatment effect on the microstructure, tensile properties and dry sliding wear behavior of A356–10%B_4C cast composites. Mater Des 31(9):4414–4422
29. Hosseini N, Karimzadeh F, Abbasi MH, Enayati MH (2010) Tribological properties of Al6061–Al_2O_3 nanocomposite prepared by milling and hot pressing. Mater Des 31(10):4777–4785
30. Rao RN, Das S (2010) Effect of matrix alloy and influence of SiC particle on the sliding wear characteristics of aluminium alloy composites. Mater Des 31(3):1200–1207
31. Balaji V, Sateesh N, Hussain MM (2015) Manufacture of aluminium metal matrix composite (Al7075–SiC) by stir casting technique. Mater Today Proc 2:3403–3408
32. Satyanarayana T, Rao PS, Gopi Krishna M (2019) Influence of wear parameters on friction performance of A356 aluminum–graphite/granite particles reinforced metal matrix hybrid composites. Heliyon 5:e01770
33. Harichandran R, Selvakumar N (2015) Effect of nano/micro B_4C particles on the mechanical properties of aluminium metal

matrix composites fabricated by ultrasonic cavitation-assisted solidification process. Arch Civ Mech Eng 6:1–12
34. ASTM B557M-07 (2007) Standard test methods for tension testing wrought and cast aluminum- and magnesium-alloy products [metric]. ASTM International, West Conshohocken, PA. www.astm.org
35. IS 1599 (2012) Metallic materials—bend test, 2012
36. IS 1757 (1988) Method for Charpy impact test (V notch) for metallic material
37. IS 1501 (2002) Method For Vickers hardness test for metallic materials
38. ASTM B831-05 (2005) Standard test method for shear testing of thin aluminum alloy products. ASTM International, West Conshohocken, PA. www.astm.org
39. ASTM G99-17 (2017) standard test method for wear testing with a pin-on-disk apparatus. ASTM International, West Conshohocken, PA. www.astm.org
40. Shirvanimoghaddam K et al (2016) Boron carbide reinforced aluminium matrix composite: physical, mechanical characterization and mathematical modelling. Mater Sci Eng A 658:135–149
41. Shukla M, Dhakad SK, Agarwal P, Pradhan MK (2018) Characteristic behaviour of aluminium metal matrix composites: a review. Mater Today Proc 5(2, Part 1):5830–5836
42. Kumar KR, Kiran K, Sreebalaji VS (2017) Micro structural characteristics and mechanical behaviour of aluminium matrix composites reinforced with titanium carbide. J Alloy Compd 723:795–801
43. Ghasali E et al (2015) Investigation on microstructural and mechanical properties of B_4C–aluminum matrix composites prepared by microwave sintering. J Mater Res Technol 4(4):411–415
44. Nassar AE, Nassar EE (2017) Properties of aluminum matrix nano composites prepared by powder metallurgy processing. J King Saud Univ Eng Sci 29(3):295–299
45. Alam SN, Kumar L (2016) Mechanical properties of aluminium based metal matrix composites reinforced with graphite nanoplatelets. Mater Sci Eng A 667:16–32
46. Harichandran R, Selvakumar N (2016) Effect of nano/micro B_4C particles on the mechanical properties of aluminium metal matrix composites fabricated by ultrasonic cavitation-assisted solidification process. Arch Civ Mech Eng 16(1):147–158
47. Thévenot F (1990) Boron carbide—a comprehensive review. J Eur Ceram Soc 6(4):205–225
48. Walczak M, Pieniak D, Zwierzchowski M (2015) The tribological characteristics of SiC particle reinforced aluminium composites. Arch Civ Mech Eng 15(1):116–123
49. Raj R, Thakur DG (2016) Qualitative and quantitative assessment of microstructure in Al–B_4C metal matrix composite processed by modified stir casting technique. Arch Civ Mech Eng 16(4):949–960
50. Shirvanimoghaddam K, Khayyam H, Abdizadeh H, Akbari MK, Pakseresht AH, Abdi F, Abbasi A, Naebe M (2016) Effect of B_4C, TiB_2 and $ZrSiO_4$ ceramic particles on mechanical properties of aluminium matrix composites: experimental investigation and predictive modelling. Ceram Int 42(5):6206–6220
51. Hynes NRJ, Kumar R (2018) Electrochemical machining of aluminium metal matrix composites. Surf Eng Appl Electrochem 54(4):367–373
52. Hynes NRJ, VivekPrabhu M, Nagaraj P (2017) Joining of hybrid AA6063–6SiCp–3Grp composite and AISI 1030 steel by friction welding. Def Technol 13(5):338–345